NJC

ROYAL SOCIETY OF CHEMISTRY

PAPER

View Article Online
View Journal | View Issue

Cite this: *New J. Chem.*, 2020, 44, 354

Insight into the molecular mechanism that controls the solubility of CH_4 in ionic liquids†

Kiki Adi Kurnia,*[a] Choo Jia How,[b] Pranesh Matheswaran,[b] Mohd. Hilmi Noh*[bc] and M. Amin Alamsjah[a]

The solubility of methane (CH_4) in ionic liquids (ILs) is required in order to develop processes involving CH_4, such as methane conversion and CO_2/CH_4 separation from natural gas or biogas processes. Nevertheless, the solubility of CH_4 in ILs is still very rarely achieved and, consequently, fundamental knowledge about the factors that govern the solubility are still poorly understood. Therefore, this work aims to extend the solubility data of CH_4 in various ILs and to gain some insights into the factors at a molecular level that play a role in the solubility process through experimental and computational modelling using Conductor-like Screening Model for Real Solvent (COSMO-RS). The solubility of CH_4 in 17 commercial ILs was measured experimentally at four different temperatures (298.15 to 343.15 K) and pressures up to 8 MPa. The large number of ILs studied allows the study of the impact of the cation and anion head group and the alkyl chain length on the solubility of CH_4. From the experimental solubility data collected, Henry's law constant (K_H) values were calculated. The results show that the solubility of CH_4 increases with decreasing temperature and increasing pressure. The solubility of CH_4 can also be enhanced by increasing the alkyl chain length of the IL cation or anion. Despite the inability of COSMO-RS to make quantitative predictions, the model is able to predict accurately the impact of the IL cation head group, anion, and alkyl chain length on the solubility of CH_4. Good correlation between the electrostatic – misfit energy, $H_{E,MF}$, of CH_4 and the experimentally calculated K_H values was obtained (R^2 = 0.932). This correlation indicates, for the first time, that the electrostatic – misfit energy arising from the repulsive interaction of CH_4 plays a dominant role in determining its solubility in ILs. In addition, it is shown that the IL size and van der Waals forces only have marginal influences on the solubility of CH_4. The experimental and computational modelling results in this work could pave the way to designing ILs as a medium for gas absorption and separation involving CH_4.

Received 2nd October 2019,
Accepted 20th November 2019

DOI: 10.1039/c9nj04973h

rsc.li/njc

Introduction

Ionic liquids (ILs) are salts with a low melting point, thus at ambient conditions they exist as a liquid and are comprised entirely of cations and anions. Due to their negligible vapor pressure and higher heats of vaporization as compared to volatile organic compounds (VOCs),[1] ILs are considered to be "green solvents". In addition, ILs have an additional array of unique physico-chemical properties such as high ionic conductivity, high thermal stability, wide liquidus range, and non-flammability. Nonetheless, a key feature of ILs is the possibility to design their physico-chemical properties with an appropriate combination of cations and anions. It is evident that the large number of possible cations and anions to form ILs provides unique opportunities to tailor the properties of these fluids for numerous applications.[2,3] A promising application may be the capture of greenhouse gases such as methane, CH_4. The first reported data on CH_4 solubility in ILs can be traced back to 2002, where Brennecke and co-workers reported the solubilities and thermodynamic properties of several gases in the IL 1-butyl-3-methylimidazolium hexafluorophosphate, $[C_4C_1im][PF_6]$.[4] They found that the solubility of CH_4 in the IL (Henry's law constant, K_H at 298.15 K = 169 MPa) was significantly lower than CO_2 (K_H at 298.15 K = 5.34 MPa), making this liquid suitable for the separation of CO_2/CH_4. Other authors have also supported the lower solubility of CH_4 as compared to CO_2 in any given IL.[5–9] Since then, ILs have been studied as a potential medium for CO_2/CH_4 separation, not only in a pure

[a] *Department of Marine, Faculty of Fisheries and Marine, Universitas Airlangga, Jalan Mulyorejo Kampus C, Surabaya, 60115, Indonesia. E-mail: kiki.adi@fpk.unair.ac.id*
[b] *Chemical Engineering Department, Universiti Teknologi PETRONAS, Bandar Seri Iskandar, Perak 32610, Malaysia. E-mail: hilmi.noh@utp.edu.my*
[c] *Center of Research in Ionic Liquids, Universiti Teknologi PETRONAS, Bandar Seri Iskandar, Perak 32610, Malaysia*

† Electronic supplementary information (ESI) available: List of ionic liquids, experimental and predicted solubilities of CH_4 in ionic liquid using COSMO-RS, and predicted volumes of ionic liquids and excess enthalpies of ionic liquid + CH_4 binary mixtures using COSMO-RS. See DOI: 10.1039/c9nj04973h

state but also in the form of a supported IL membrane,[10–12] which could be applied in natural gas sweetening or biogas upgrading.[13,14] However, it should be highlighted that while extensive research has been performed on CO_2 solubility in ILs,[15] only limited data are available on the solubility of CH_4 in these liquids.[4–9,16–22]

Recently, in addition to being solvents for the CO_2/CH_4 separation process, ILs have also been studied as a medium for conversion of methane to methanol through the oxidation reaction.[23] Li and co-workers demonstrated that the catalyst used and the ILs could be recycled several times and the conversion of CH_4 in the recycled system still maintains a high level.[23] The use of IL as a solvent for conversion of CH_4 does not only eliminate the emission of toxic organic solvents, but also will optimize the CH_4 utilization processes. Whether ILs are used as a solvent for the CO_2/CH_4 separation process or as a solvent for conversion of CH_4, understanding the solubility of CH_4 in ILs is vital for the design of the industrial absorption process involving this gas. In addition, the large amount of cations and anions has led researchers to an era where general theories need to be developed to comprehensively explain and forecast the IL phase behaviour based on the interaction with a solute of interest rather than just studying individual ILs and isolated mixtures. A unified understanding allows researchers to systematically design ILs for any target applications. Unfortunately, the solubility data of CH_4 in ILs is still very scarce, especially when compared to CO_2. The scarce data means the molecular mechanism behind CH_4 dissolution into ILs is still poorly understood.

Therefore, this work was carried out with two main objectives. First, to provide the solubility data of CH_4 in ILs and second, to gain insight into the molecular mechanism that controls the solubility of CH_4 in ILs. To achieve these objectives, the solubility of CH_4 in a large number of ILs was measured using high pressure gas solubility at four different temperatures (298.15, 313.15, 328.15, and 343.15 K) and pressures up to 8 MPa. The selected ILs cover common imidazolium, pyridinium, piperidinium, and pyrrolidinium, which are combined with a wide variation of anion. The broad range of ILs allows systematic analysis of the impact of ILs structure, such as cation head group, anion head group, and cation/anion alkyl chain length on the solubility of CH_4. The experimental data is also accompanied with computational modelling, namely Conductor like Screening Model for Real Solvent (COSMO-RS). The computational modelling result can compensate for some shortcomings of the experiments and provide information on the relationship between the ILs electronic/chemical structures and the solubility of CH_4 on these ILs. That way, the investigations based on the electronic level provide a more direct understanding of the intra- and intermolecular interactions between ILs and CH_4.

Methodology

Chemicals

High purity gases, namely CH_4 (99.5 wt%) and N_2 (99.0 wt%) were supplied by Mox-Linde Gases Sdn. Bhd. Table S1 in the ESI† provides a list of the wide variety of ILs used in this study along with their general information. All gases and ILs were used as received from the supplier without any further purification.

Measurement of CH_4 Solubility

The solubilities of CH_4 in ILs were measured using a High Pressure Gas Solubility Cell (SOLTEQ, Model: BP 22), similar to our previous work.[24,25] This equipment consists of two main vessels, namely mixing and equilibrium vessels. Both vessels were equipped with a digital pressure indicator (Druck DPI 150) with a precision of ±0.001 kPa for a range of (0 to 10 MPa) and a digital thermometer (YOKOGAWA 7653) with a precision of ±0.01 K. Prior to the experimental measurements, both vessels were purged with nitrogen gas and evacuated to a pressure of <0.005 MPa. A known amount of IL, *circa* 5 g, was then fed into the equilibrium vessel, whereas the CH_4 gas was injected into the mixing vessel, *circa* 8–9 MPa. The apparatus was brought to a desired temperature and CH_4 gas was then introduced to the equilibrium vessel from the mixing vessel. Throughout the absorption process, the solution was continuously stirred with a magnetic stirrer to optimize the solubility in the system. The temperature of the system was maintained using a JULABO thermostatic water circulator with the uncertainty ±0.1 K. When the pressure of the equilibrium vessel reached a constant value, then the equilibrium was assumed to be attained. The amount of CH_4 gas dissolved in IL was calculated using the following equation:

$$n_{gas} = \frac{V_e}{RT_e}\left(\frac{p_i}{Z_i} - \frac{p_e}{Z_e}\right) \quad (1)$$

where V_e denotes the volume of equilibrium vessel, Z_i and Z_e are the compressibility factors corresponding to the initial and equilibrium pressure, p_i and p_e, respectively. T_e is the temperature at equilibrium, whereas R is the universal gas constant.

The CH_4 solubility results are presented in terms of mole fraction of the gas dissolved in ILs and are calculated using eqn (2),

$$x_{gas} = \frac{n_{gas}}{n_{gas} + n_{IL}} \quad (2)$$

where n_{gas} is the amount of CH_4 dissolved in IL and n_{IL} is the amount of IL. Alternatively, the solubility of CH_4 can also be expressed as Henry's law constant, K_H, which is defined as,

$$K_H(p, T, x_{gas}) = \lim_{x_{gas}\to 0} \frac{f_2(p, T, x_{gas})}{x_{gas}} \quad (3)$$

where f_2 is the fugacity of CH_4 gas. Since ILs have a negligible vapor pressure, the fugacity of the gas is assumed to be equal to the pure gas, which can be expressed as,

$$f_2(p,T) = p_{eq}\,\phi_2(p_{eq},T_{eq}) \quad (4)$$

where p_{eq} and T_{eq} are the pressure and temperature at equilibrium, respectively. The fugacity coefficient, ϕ_2, is calculated using the Peng–Robinson equation of state. Combining eqn (3) and (4) produces,

$$K_H(p, T, x_{gas}) \cong \frac{\phi_2(p_e, T_e)p_e}{x_{gas}} \quad (5)$$

Computational modelling using COSMO-RS

Conductor-like Screening Model for Real Solvent (COSMO-RS) is an efficient computational modelling tool for the prediction of the thermophysical data of a pure liquid and their mixture based on unimolecular quantum chemical calculations. Unlike other prediction methods, such as Neural network,[26] the Group Contribution equation of state developed by Skjold-Jørgensen,[8] and the Peng–Robinson equation of state[27,28] which need experimental data, COSMO-RS only requires the chemical structures of the compound of interest. In addition, COSMO-RS is also able to provide insight into the molecular mechanism existence in the system of interest. Hardacre and co-workers have demonstrated that COSMOthermX is capable of qualitatively predicting solubilities of several gases in ILs.[29] However, the authors did not describe the impact of the ILs' chemical structures on the solubilities of gases.

The COSMO-RS calculation consists of two major steps. In the first step, the continuum solvation COSMO calculation of electronic density and molecular geometry of the IL cation, anion, and CH_4 were optimized using the TURBOMOLE V7.3 2018 software program package based on the density functional theory level, utilizing the BP functional B88-P86 with a triple-ζ valence polarized basis set (TZVP) and the resolution of identity standard (RI) approximation.[30] Once the COSMO file is produced, it can be stored in the database and is ready to be used for the next step. In the second step, the thermophysical properties, namely the solubility of CH_4 in ILs, and excess enthalpies of (IL + CH_4) were determined by means of the COSMO*therm* software using the parameter BP_TZVP_C30_1701 (COSMOlogic, Levekusen, Germany).[31] Unless otherwise stated, the ILs are always treated as a one to one cation/anion mixture, and the ions are treated at the quantum chemical level separately, and therefore, it is possible to analyze the contribution of cations and anions to the predicted properties. The details of the COSMO-RS calculation on estimating the chemical potential is given in the COSMOtherm User's Manual.[31]

In brief, the solubility of CH_4 in the IL is calculated in an iterative procedure. For each compound j, the mole fraction, x_j, is varied until the partial pressure of the compound is equal to the given reference pressure, P, according to eqn (6),

$$P_j = P_j^0 x_j \gamma_j \tag{6}$$

where P_j^0 is the vapor pressure of the pure compound j and γ_j is the activity coefficient of gas in solvent.

The most important output from the COSMO-RS model is the interaction energies of the pure IL and CH_4 molecules. Thus, the COSMO-RS model allows both chemical structure and interactions to be probed on a molecular level providing vital information on the impact of structural changes upon the solubility process. In the molecular approach, the COSMO-RS model focuses on three specific interactions, namely the electrostatic – misfit energy, H_{MF}, hydrogen bonding energy, H_{HB}, and van der Waals energy, H_{vdW}. These energies are described in eqn (7)–(9), respectively:

$$H_{MF} = a_{eff}\frac{\alpha}{2}(\sigma + \sigma')^2 \tag{7}$$

$$H_{HB} = a_{eff}c_{HB}(0; \min(0; \sigma_{donor} + \sigma_{HB}) \times \max(0; \sigma_{acceptor} + \sigma_{HB})) \tag{8}$$

$$H_{vdW} = a_{eff}(\tau_{vdW} + \tau_{vdW}') \tag{9}$$

where a_{eff} is the effective contact area between two surface segments, α' is the interaction parameter, σ_{HB} is the hydrogen bond strength that is the threshold for hydrogen bonding, and the last two τ_{vdw} and τ_{vdw}' are elements of specific van der Waals interaction parameters.

In addition, interaction energies between ILs–CH_4 were also estimated by COSMO-RS using the excess enthalpies as the difference in the enthalpy of the studied cation, anion, or CH_4 molecules in its mixture and pure state, according to the following equation:

$$H_{E,i}(\text{interaction}) = H_{i,mixture}(\text{interaction}) - H_{i,pure}(\text{interaction}) \tag{10}$$

The $H_{E,i}$ (interaction) in the COSMO-RS model originates from a total summation of the three specific interaction as described in eqn (7)–(9). Thus, it can be expressed as,

$$H_{E,m} = H_{E,MF} + H_{E,HB} + H_{E,vdW} \tag{11}$$

Therefore, the COSMO-RS model could provide the information required for the evaluation of molecular interaction of ILs occurred in the pure state, as well as in the (ILs + CH_4) binary mixtures.

Results and discussion

The experimental and predicted solubility data of CH_4 in ILs using COSMO-RS is given in Table S2 in the ESI.† The solubility data provided is for temperatures ranging from 298.15 to 343.15 K with 15 K intervals and pressures up to 8 MPa. The comparison between the recorded data in this work and those already reported in the literature is given in Fig. S1 to S4 in the ESI.† Due to the difference in the temperature measured in this work and the references, the comparison is made by the closest temperature between these two data sets. Good agreement of CH_4 solubility in 1-butyl-3-methylimidazolium methylsulphate, $[C_4C_1im][MeSO_4]$, is reported in this work and also in the literature.[19] For the ILs containing the $[Tf_2N]$ anion, the acquired solubility data in this work is relatively lower than those in the literature data.[6,18,28] One main exception was found for the data reported by Liu and co-workers,[32] where a higher deviation was observed for $[C_2C_1im][Tf_2N]$. This higher deviation may be attributed to either the purity of the samples that the author did not mention or the use of a different experimental setup that requires density data.[32] Nevertheless, in general, the solubility data obtained in this work are in good agreement with most of the published data.[6,18,19,28]

An example of a typical phase diagram describing the solubility of CH_4 in ILs is displayed in Fig. 1. In general, the solubility of CH_4 increases with the increase of pressure and decreases with the increase of temperature, with the former having a more significant influence. The minor effect of temperature on the solubility of CH_4 in IL has been reported by other authors.[6,33]

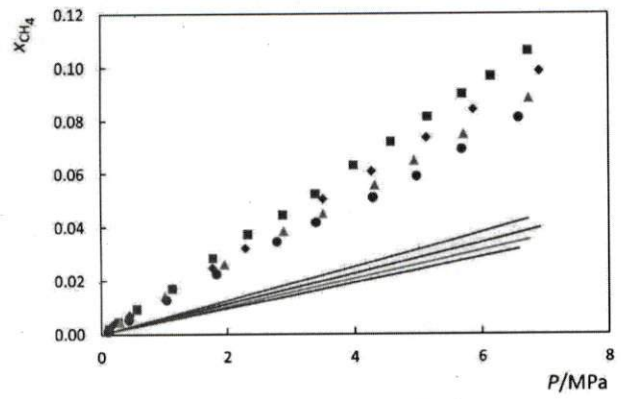

Fig. 1 Solubility of CH_4, x_{CH_4}, in IL $[C_4C_1im][Tf_2N]$ as a function of pressure, P, at different temperatures. Symbols: (■), 298.15 K; (♦), 313.15 K; (▲), 328.15; and (●), 343.15 K. The lines represent the COSMO-RS prediction data.

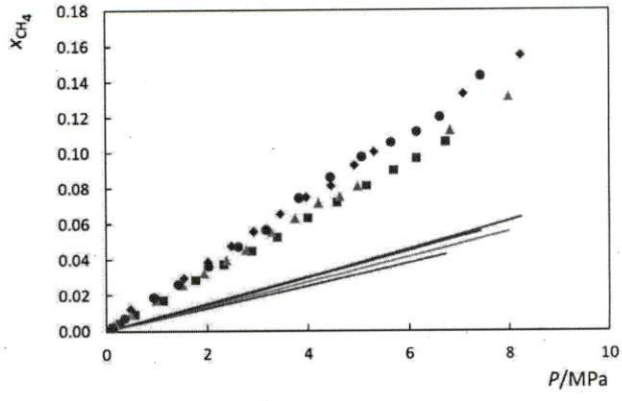

Fig. 2 Solubility of CH_4, x_{CH_4}, in ILs with different cation head groups as a function of pressure, P, at the temperature 298.15 K. Symbols: (■), $[C_4C_1im][Tf_2N]$; (♦), $[C_4C_1py][Tf_2N]$; (▲), $[C_4C_1pyrr][Tf_2N]$; and (●), $[C_4C_1pip][Tf_2N]$. The lines represent the COSMO-RS prediction data.

With regard to COSMO-RS, generally, the model underestimates the solubility of CH_4 in ILs, but still in a reasonable magnitude. The temperature–pressure dependence of the solubility of CH_4 in IL is also well predicted, qualitatively, by COSMO-RS. In this regard, despite the inability of the model to predict accurately the solubility of CH_4 in the IL, COSMO-RS was able to provide the impact of pressure and temperature. The same observation is also observed by Hardacre and co-workers.[29] The authors proposed that a better prediction might be obtained for gases when using experimental correlations such as the Antoine or Wagner equation. Nevertheless, the main point to highlight here is that COSMO-RS could qualitatively predict the gas solubility in ILs in a similar order of magnitude when compared with the experimental data, and other features that will be discussed below.

Effect of IL structure

The large amount of experimental data reported in Table S2 in the ESI,† allows us to study the effect of the IL structure on the solubility of CH_4. The structural factors, such as the cation and anion head group, aromaticity and chain length are analysed and discussed in term of their impact on the solubility of CH_4. By fixing the anion and alkyl chain length, it is possible to study the impact of the cation head group, namely imidazolium, pyridinium, piperidinium, and pyrrolidinium on the solubility of CH_4, as depicted in Fig. 2. This reveals that the increase of CH_4 solubility at 298.15 K follows the cation trend: $[C_4C_1im]^+ < [C_4C_1pyrr]^+ < [C_4C_1py]^+ \approx [C_4C_1pip]^+$. The same trend is also observed at different temperatures studied. From the trend, it is noticeable that solubility of CH_4 is higher in the six-member ring cation (pyridinium and piperidinium) than in the five-member ring cation (imidazolium and pyrrolidinium). Since both imidazolium and pyridinium are aromatic cations, while the other two are not, it can be projected that the IL cation size is more influential than the aromaticity in defining the solubility of CH_4. The improved solubility might be due to the increase in IL size that enhances the probability of favourable dispersive interactions with CH_4.

In regard to COSMO-RS, despite the inability to accurately predict the solubility quantitatively, the model is capable of correctly predicting the rank of IL cation on the solubility of CH_4, similar to the experimental observation. From a chemical engineering perspective, this information is useful and practical in understanding the trend of gas solubility with different IL cations and anions.

The cation alkyl chain length also affects the solubility of CH_4 in the ILs. Fig. 3 depicts the solubility of CH_4 in a series of ILs $[C_nC_1im][Tf_2N]$, where n is 1, 2, 4, 6, and 10, at 298.15 and pressure is up to 8 MPa. Indeed, significant solubility variation of CH_4 in ILs with different cation alkyl chain lengths can be observed in Fig. 3. The solubility of CH_4 in this series of ILs can be ranked as follows: $[C_1C_1im][Tf_2N] < [C_2C_1im][Tf_2N] < [C_4C_1im][Tf_2N] < [C_6C_1im][Tf_2N] < [C_{10}C_1im][Tf_2N]$. This ranking is also supported by their estimated K_H values, as depicted in Table 1. Mutelet and co-workers[34] also observed that the solubility of CH_4 in $[C_4C_1im][Tf_2N]$ was higher than in $[C_2C_1im][Tf_2N]$, in concordance with the results in this work. The significant improvement of the solubility of CH_4 with the increase of alkyl chain length supports the previous premise that IL size has

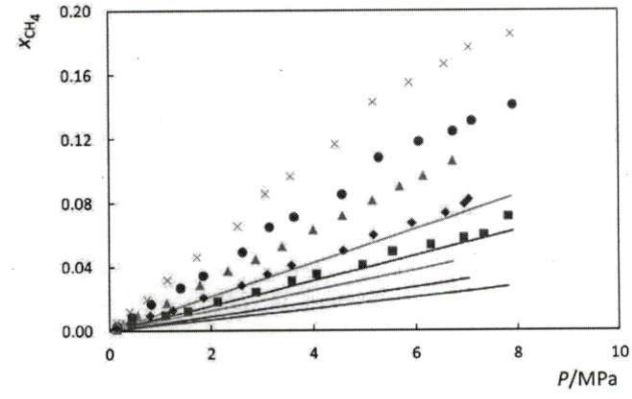

Fig. 3 Solubility of CH_4, x_{CH_4}, in ILs with different cation alkyl chain lengths as a function of pressure, P, at temperature 298.15 K. Symbols: (■), $[C_1C_1im][Tf_2N]$; (♦), $[C_2C_1im][Tf_2N]$; (▲), $[C_4C_1im][Tf_2N]$; (●), $[C_6C_1im][Tf_2N]$; and (×), $[C_{10}C_1im][Tf_2N]$. The lines represent the COSMO-RS prediction data.

Table 1 Henry's law constant, K_H, values of CH_4 in ILs at different temperatures

Ionic liquid	K_H/MPa			
	298.15 K	313.15 K	328.15 K	343.15 K
$[C_4C_1im][Ac]$	53.21	64.69	78.20	90.22
$[C_4C_1im][BF_4]$	116.89	131.36	150.54	165.49
$[C_4C_1im][DMP]$	55.11	66.03	78.71	89.06
$[C_4C_1im][DBP]$	40.17	46.29	54.27	61.40
$[C_4C_1im][PF_6]$	111.78	123.10	134.49	141.60
$[C_4C_1im][SCN]$	106.01	122.97	142.08	153.57
$[C_4C_1im][MeSO_4]$	157.99	182.39	213.21	238.21
$[C_4C_1im][OcSO_4]$	42.37	50.60	59.02	65.73
$[C_4C_1im][TFA]$	75.17	89.58	103.98	117.46
$[C_4C_1im][Tf_2N]$	55.92	62.80	69.82	75.24
$[C_4C_1pip][Tf_2N]$	46.35	51.99	57.60	64.66
$[C_4C_1pyrr][Tf_2N]$	53.03	59.20	63.67	69.76
$[C_4C_1py][Tf_2N]$	46.17	52.79	59.00	65.18
$[C_1C_1im][Tf_2N]$	99.05	109.35	116.21	123.85
$[C_2C_1im][Tf_2N]$	76.08	84.64	92.78	99.83
$[C_6C_1im][Tf_2N]$	46.68	50.46	56.60	61.91
$[C_{10}C_1im][Tf_2N]$	34.99	37.99	42.51	47.71

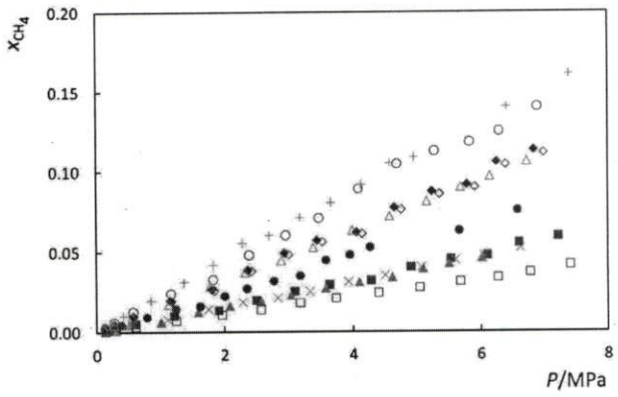

Fig. 4 Solubility of CH_4, x_{CH_4}, in ILs with different anions as a function of pressure, P, at a temperature of 298.15 K. Symbols: (■), $[C_4C_1im][SCN]$; (♦), $[C_4C_1im][Ac]$; (▲), $[C_4C_1im][BF_4]$; (●), $[C_4C_1im][TFA]$; (×), $[C_4C_1im][PF_6]$; (□), $[C_4C_1im][MeSO4]$; (◊), $[C_4C_1im][DMP]$; (△), $[C_4C_1im][Tf_2N]$; (○), $[C_4C_1im][OcSO4]$, and (+), $[C_4C_1im][DBP]$.

more effect on the solubility. COSMO-RS is also able to forecast the impact of cation alkyl chain length on the solubility of CH_4 as observed experimentally.

The increase of solubility of CO_2 is also observed with the increase of cation alkyl chain length but marginally.[35,36] Whereas, in this work, it is shown that cation alkyl chain length has a higher impact toward the solubility of CH_4. This information is very important in the screening and selection of ILs with high CO_2/CH_4 selectivity. In this regard, increasing alkyl chain length leads to an increase of solubility of CO_2 only slightly and CH_4 substantially. As a result, ILs with a long alkyl chain length may have a higher solubility of CH_4 and consequently, it has low CO_2/CH_4 selectivity.

Substantial variation of CH_4 solubility is also observed in a series of ILs $[C_4C_1im]$ with different anions, as depicted in Fig. 4. Aiming to get a clear picture on the impact of the IL anion toward the solubility of CH_4 experimentally, the COSMO-RS prediction is given separately in Fig. S5 in the ESI.† Several points could be extracted from Fig. 4. First, the increase of anion alkyl chain length, as in the case of $[C_4C_1im][MeSO_4]$ to $[C_4C_1im][OcSO_4]$ and from $[C_4C_1im][DMP]$ to $[C_4C_1im][DBP]$, leads to an increase of CH_4 solubility. This result could be due to the increase in the non-polar character of the ILs, and consequently, could increase the possibility of favourable dispersive interactions with CH_4, as observed with the cation alkyl chain length. Second, on the contrary, the increase of the IL anion size from $[C_4C_1im][Ac]$ (molecular volume predicted using COSMO-RS, $V_{m,COSMO}$ = 0.2721 nm^3) to $[C_4C_1im][TFA]$ ($V_{m,COSMO}$ = 0.2954 nm^3) unfortunately leads to a decrease in the solubility of CH_4. This peculiar observation could be due to the exclusive absorption behaviour of $[C_4C_1im][Ac]$ or an indication that solubility of CH_4 is not only governed by IL size, but also due to the existence of other molecular forces. For example, the solubility of CO_2 is not only ruled by IL size but also, arguably, controlled by IL anion basicity.[37,38] However, the solubility of CH_4 does not follow the IL anion basicity rank.[39] To get a better understanding on the molecular level of what controls the solubility of CH_4 in ILs, the quantum-chemical based computational modelling using COSMO-RS is discussed below.

Henry's law constant

In addition to the mole fraction, the gas solubility in IL can also be expressed in Henry's law constant, K_H, calculated using eqn (5). Table 1 lists the experimentally obtained K_H values of CH_4 in the studied ILs. In general, the trend in K_H values is similar to the gas solubility ranking. For example, the increase of temperature leads to a decrement of solubility of CH_4 in ILs that translates to an increase of K_H values. In addition, the K_H values for cations with a six-membered ring are slightly lower than in a five-membered ring which in return, supports the higher solubility of CH_4 in the former cations. The impact of alkyl chain length of the cations and anions are also well captured by their corresponding K_H values. Thus, while the obtained KH values strengthen the impact of the IL chemical structures on the solubility of CH_4, the question that remains is which type of molecular mechanism plays a role in this process.

Computational modelling using COSMO-RS

In order to gain an insight into the mechanism at the molecular level that governs the solubility of CH_4 in ILs, a detail analysis based on the COSMO-RS was carried out. Cláudio and co-workers demonstrated that the ^{1}H-NMR shifts of the cation and anion are in good agreement with the predicted energy using COSMO-RS.[39] Other works have also shown that the excess energy, predicted using COSMO-RS, is capable of providing an insight into the existence of the molecular mechanism in the system of interest.[40,41] Therefore, COSMO-RS was used in this work, aiming to gain an insight into the solubility of CH_4 in ILs, which is still poorly understood.

Based on the gathered experimental data, where size has an influence on the solubility of CH_4, the first attempt is to correlate the experimental K_H values and the predicted molecular volume of ILs using COSMO-RS, $V_{m,COSMO}$ (*cf.* Table S3 in ESI†). The plot of K_H at the temperature 298.15 K and $V_{m,COSMO}$ is given in Fig. S6 in the ESI.† Unfortunately, the plot only produces

R^2 *circa* 0.52, which indicates inadequate correlation between these two parameters. This means that IL size is not a dominant factor that governs the solubility of CH_4. Vlugt and co-workers[28] also attempted to correlate the solubility of CH_4 with IL size (in term of molecular weight). They found that the solubility data for CH_4 in ILs do not collapse on an universal absorption curve, as in the case of CO_2.[15,28] These findings further confirm that IL size is not a dominant factor that controls the solubility of CH_4.

In another approach, COSMO-RS was then used to predict the interaction, in term of excess energy, between ILs–CH_4 ($H_{E,IL\text{-}CH_4}$) and the values are given in Table S4 in the ESI.† The excess energy was estimated at x_{gas} = 0.01, as CH_4 is soluble in all studied ILs in this concentration. The estimated excess energy shows that, interestingly, the attractive interaction (represented by a negative value) arises from the IL cation, which is an electrostatic misfit and, to a small extent, the van der Waals forces. The hydrogen bonding between the cation and CH_4, as expected, is nil, as the latter does not have the capability to act as a hydrogen bond donor or acceptor. It is also thought-provoking to highlight that, in general, the IL anion contributes highly to the endothermicity of the (IL + CH_4) system. Several correlations were attempted between the predicted excess energy and experimental K_H values. Remarkably, the plot of $H_{E,MF}$ as the contribution of CH_4 against K_H, produces a satisfying correlation coefficient, 0.932, as depicted in Fig. 5. Accordingly, the conclusion can be drawn that the electrostatic – misfit interaction arose from the CH_4 molecule, which controls its solubility in ILs. Due to the non-polar nature of CH_4, it is expected that this molecule will cease interacting with high-density charge fragment of ILs, which are the cation and anion head groups. The interaction is predictable and will occur within the non-polar region of the ILs, which is the alkyl chain length. A longer alkyl chain is preferred by a CH_4 molecule as it keeps away from the highly charged IL head. This explains the significant influence of the alkyl chain length toward the solubility of CH_4 in ILs.

Thus, the scenario of CH_4 solubility in the ILs can be described as follows (i) the addition of the CH_4 molecule leads to the rupture of the hydrogen bonding between the IL cation and anion, as indicated by the positive values of $H_{E,HB}$. This process is then followed by (ii) the establishment of a new attractive electrostatic – misfit interaction between the CH_4 – cation. In some specific cases, for example, with an anion with a long alkyl chain, such as $[DBP]^-$ and $[OcSO_4]^-$, a favourable interaction with CH_4 is also observed, as indicated by the negative $H_{E,MF}$ of the respective anion. The dominant electrostatic – misfit interaction is found to be responsible for enhancing the solubility of CH_4 with increasing alkyl chain length and increasing the size of the cation head group, from a 5-membered to a 6-membered ring. Therefore, the COSMO-RS method can be used to modulate and interpret the excess enthalpies considering the contribution of the specific interactions that occur between each species (molecules and ions), and ultimately, to understand the solubility of CH_4 in ILs at the molecular level.

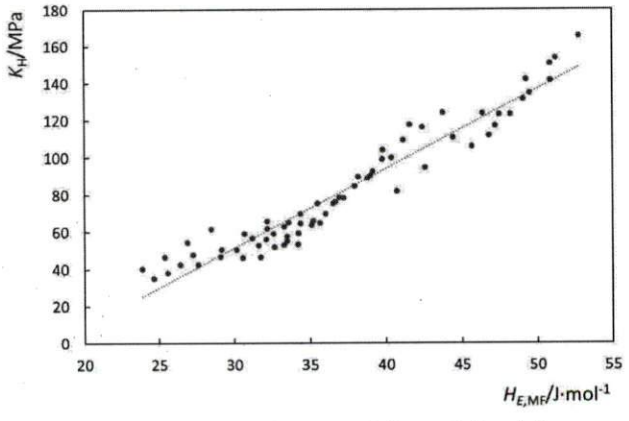

Fig. 5 Plot of excess enthalpy in terms of electrostatic-misfit as a contribution of CH_4 in the (IL + CH_4) binary system, $H_{E,MF}$, predicted using COSMO-RS against the experimentally calculated Henry's law constants of CH_4 in ILs, K_H, at different temperatures.

Conclusions

In this work, the solubility of CH_4 in a large number of ILs was measured experimentally at four different temperatures (298.15, 313.15, 328.15, and 343.15 K) and at pressures up to 8 MPa. Henry's law constants were calculated from the recorded experimental solubility data. The gathered results show that the solubility of CH_4 in ILs increases with a decrease in temperature and an increase in pressure. In addition, an improvement in CH_4 solubility could also be achieved with an increase in the alkyl chain length of the IL cation or anion. Furthermore, it is shown here for the first time that the solubility of CH_4 is highly controlled by the electrostatic-misfit interaction of CH_4 with the IL cation, while the van der Waals forces due to the cation contribute slightly. In summary, combining experimental and computational modelling approaches for a large number of ILs could give important insights into the mechanism that controls the solubility of CH_4 in room temperature molten salts. The gathered data in this work could be used to pave the way to design an IL with optimized CH_4 solubility.

Conflicts of interest

There are no conflicts to declare.

Acknowledgements

This work is supported by a Fundamental Research Grant from Yayasan Universiti Teknologi PETRONAS (reference number: YUTP/2016/0153AA-E31) and Hibah Paper Review from Universitas Airlangga.

References

1 J. P. Armstrong, C. Hurst, R. G. Jones, P. Licence, K. R. J. Lovelock, C. J. Satterley and I. J. Villar-Garcia, *Phys. Chem. Chem. Phys.*, 2007, **9**, 982–990.

2 N. V. Plechkova and K. R. Seddon, *Ionic Liquids Uncoiled - Critical Expert Overviews*, A John Wiley & Sons, Inc., Publication, 2013.

3 W. Wang, X. Ma, S. Grimes, H. Cai and M. Zhang, *Chem. Eng. J.*, 2017, **328**, 353–359.
4 J. L. Anthony, E. J. Maginn and J. F. Brennecke, *J. Phys. Chem. B*, 2002, **106**, 7315–7320.
5 D. Morgan, L. Ferguson and P. Scovazzo, *Ind. Eng. Chem. Res.*, 2005, **44**, 4815–4823.
6 P. J. Carvalho and J. A. P. Coutinho, *Energy Environ. Sci.*, 2011, **4**, 4614–4619.
7 M. Althuluth, M. C. Kroon and C. J. Peters, *Ind. Eng. Chem. Res.*, 2012, **51**, 16709–16712.
8 M. D. Bermejo, T. M. Fieback and Á. Martín, *J. Chem. Thermodyn.*, 2013, **58**, 237–244.
9 M. Götz, F. Ortloff, R. Reimert, O. Basha, B. I. Morsi and T. Kolb, *Energy Fuels*, 2013, **27**, 4705–4716.
10 D. Camper, J. Bara, C. Koval and R. Noble, *Ind. Eng. Chem. Res.*, 2006, **45**, 6279–6283.
11 J. E. Bara, D. L. Gin and R. D. Noble, *Ind. Eng. Chem. Res.*, 2008, **47**, 9919–9924.
12 J. E. Bara, R. D. Noble and D. L. Gin, *Ind. Eng. Chem. Res.*, 2009, **48**, 4607–4610.
13 J. Haider, M. A. Qyyum, B. Kazmi, M. Zahoor and M. Lee, *J. Cleaner Prod.*, 2019, **231**, 953–962.
14 Y. Xie, J. Björkmalm, C. Ma, K. Willquist, J. Yngvesson, O. Wallberg and X. Ji, *Appl. Energy*, 2018, **227**, 742–750.
15 P. J. Carvalho, K. A. Kurnia and J. A. P. Coutinho, *Phys. Chem. Chem. Phys.*, 2016, **18**, 14757–14771.
16 Y. Kou, W. Xiong, G. Tao, H. Liu and T. Wang, *J. Nat. Gas Chem.*, 2006, **15**, 282–286.
17 X. Yuan, S. Zhang, Y. Chen, X. Lu, W. Dai and R. Mori, *J. Chem. Eng. Data*, 2006, **51**, 645–647.
18 J. Kumełan, Á. P.-S. Kamps, D. Tuma and G. Maurer, *Ind. Eng. Chem. Res.*, 2007, **46**, 8236–8240.
19 J. Kumełan, Á. P.-S. Kamps, D. Tuma and G. Maurer, *J. Chem. Eng. Data*, 2007, **52**, 2319–2324.
20 X. Liu, W. Afzal, G. Yu, M. He and J. M. Prausnitz, *J. Phys. Chem. B*, 2013, **117**, 10534–10539.
21 L. M. C. Pereira, M. B. Oliveira, A. M. A. Dias, F. Llovell, L. F. Vega, P. J. Carvalho and J. A. P. Coutinho, *Int. J. Greenhouse Gas Control*, 2013, **19**, 299–309.
22 M. T. Mota-Martinez, M. Althuluth, A. Berrouk, M. C. Kroon and C. J. Peters, *Fluid Phase Equilib.*, 2014, **362**, 96–101.
23 T. Li, S. J. Wang, C. S. Yu, Y. C. Ma, K. L. Li and L. W. Lin, *Appl. Catal., A*, 2011, **398**, 150–154.
24 K. A. Kurnia, F. Harris, C. D. Wilfred, M. I. Abdul Mutalib and T. Murugesan, *J. Chem. Thermodyn.*, 2009, **41**, 1069–1073.
25 F. Harris, K. A. Kurnia, M. I. A. Mutalib and M. Thanapalan, *J. Chem. Eng. Data*, 2009, **54**, 144–147.
26 M. Safamirzaei and H. Modarress, *Fluid Phase Equilib.*, 2012, **332**, 165–172.
27 M. Althuluth, A. Berrouk, M. C. Kroon and C. J. Peters, *Ind. Eng. Chem. Res.*, 2014, **53**, 11818–11821.
28 M. Ramdin, A. Amplianitis, S. Bazhenov, A. Volkov, V. Volkov, T. J. H. Vlugt and T. W. de Loos, *Ind. Eng. Chem. Res.*, 2014, **53**, 15427–15435.
29 N. A. Manan, C. Hardacre, J. Jacquemin, D. W. Rooney and T. G. A. Youngs, *J. Chem. Eng. Data*, 2009, **54**, 2005–2022.
30 TURBOMOLE V7.3 available from http://www.turbomole.com, 2018.
31 F. Eckert and A. Klamt, *COSMOtherm Version C30 Release 18*, COSMOlogic GmbH & Co. KG, Leverkusen, Germany, 2018.
32 X. Liu, W. Afzal and J. M. Prausnitz, *Ind. Eng. Chem. Res.*, 2013, **52**, 14975–14978.
33 M. Mirzaei, B. Mokhtarani, A. Badiei and A. Sharifi, *J. Chem. Thermodyn.*, 2018, **122**, 31–37.
34 Y. Chen, F. Mutelet and J.-N. Jaubert, *Fluid Phase Equilib.*, 2014, **372**, 26–33.
35 S. N. V. K. Aki, B. R. Mellein, E. M. Saurer and J. F. Brennecke, *J. Phys. Chem. B*, 2004, **108**, 20355–20365.
36 B. Mokhtarani, A. Negar Khatun, M. Mafi, A. Sharifi and M. Mirzaei, *J. Chem. Eng. Data*, 2016, **61**, 1262–1269.
37 F. Gao, Z. Wang, P. Ji and J.-P. Cheng, *Front. Chem.*, 2019, **6**, 658.
38 N. M. Simon, M. Zanatta, J. Neumann, A.-L. Girard, G. Marin, H. Stassen and J. Dupont, *ChemPhysChem*, 2018, **19**, 2879–2884.
39 A. F. M. Cláudio, L. Swift, J. P. Hallett, T. Welton, J. A. P. Coutinho and M. G. Freire, *Phys. Chem. Chem. Phys.*, 2014, **16**, 6593–6601.
40 K. A. Kurnia and J. A. P. Coutinho, *Ind. Eng. Chem. Res.*, 2013, **52**, 13862–13874.
41 J. F. B. Pereira, K. A. Kurnia, M. G. Freire, J. A. P. Coutinho and R. D. Rogers, *ChemPhysChem*, 2015, **16**, 2219–2225.

